Catalysis Today 146 (2009) 266–273

Contents lists available at ScienceDirect

Catalysis Today

journal homepage: www.elsevier.com/locate/cattod

Physicochemical origins of electrochemical promotion of LSM/YSZ

V. Roche [a,b], A. Hadjar [a], J.P. Deloume [a], T. Pagnier [b], R. Revel [c], C. Roux [b], E. Siebert [b], P. Vernoux [a,*]

[a] Université Lyon 1, CNRS, UMR 5256, IRCELYON, Institut de Recherches sur la Catalyse et l'Environnement de Lyon, 2 Avenue Albert Einstein, F-69626 Villeurbanne Cedex, France
[b] Laboratoire d'Electrochimie et de Physico-chimie des Matériaux et des Interfaces de Grenoble (LEPMI), UMR 5631 CNRS-INPG-UJF, ENSEEG, BP 75, 38402 St Martin d'Hères, France
[c] IFP-Lyon, Rond-Point de l'échangeur de Solaize, BP3, 69360 Solaize, France

ARTICLE INFO

Article history:
Available online 30 May 2009

Keywords:
EPOC
NEMCA effect
LSM
Propane oxidation
O_2-TPD
TPO
TPR
Chemisorption

ABSTRACT

A complex route provided powders of $La_{1-x}Sr_xMnO_3$ ($x = 0$, 0.15, 0.3 and 0.4) from the thermal decomposition of the chelated nitrate precursors. The catalysts were characterized by XRD, BET, SEM, and temperature-programmed techniques. Electrochemical catalysts based on $La_{0.7}Sr_{0.3}MnO_3$ (LSM) were deposited on yttria-stabilized zirconia (YSZ) pellets. Electrochemical characterizations of these samples evidenced two redox processes assigned to the existence of different environments around Mn^{4+} in LSM in good agreement with the peaks observed by temperature programmed reduction (TPR). In situ O_2 temperature programmed desorption (O_2-TPD) and temperature programmed oxidation (TPO) of propane were performed on LSM/YSZ to investigate the influence of the polarization on oxygen and propane chemisorption on LSM/YSZ. O_2-TPD experiments have shown that the electrical polarization during adsorption process has no significant impact on gaseous oxygen adsorption on LSM thin film. TPO experiments suggest an increase in the adsorption strength of propane on LSM that could be at the origin of the electrochemical promotion effects observed upon polarization conditions.

1. Introduction

Propane is a fuel of great interest as a major component of liquid petroleum gas (LPG). Its catalytic oxidation appears to be one of the crucial points for the clean production of energy [1]. Noble metal catalysts exhibit the best activity to perform this reaction. However, they present deactivation and high volatility at high operating temperatures in addition to an excessive cost [1]. To overcome these drawbacks, perovskite-type oxides with the general formula ABO_3 are proposed as alternative catalysts especially lanthanum manganites. The stability of the perovskite structure allows partial substitution on both the lanthanum (A) and manganese (B) sites. These substitutions generally enhance the activity of the catalyst [1]. Arai et al. [2] reported that $La_{0.6}Sr_{0.4}MnO_3$ materials exhibited higher activity for the methane combustion than unsubstituted $LaMnO_3$ and so did Batis et al. [4] for $La_{0.4}Ca_{0.6}MnO_3$. Many recent studies [3–6] are available to explain the modification of catalytic behaviour induced by partial substitution in the perovskite structure. For instance in case of $LaFeO_3$ catalysts Ciambelli et al. [3,6] observed a combined effect induced by the insertion of calcium on the lanthanum site attributed to the creation of oxygen vacancies and the partial oxidation of Fe^{3+} to Fe^{4+} resulting in an increase in the bulk oxygen mobility. Indeed, two mechanisms involving two kinds of oxygen species are proposed for methane oxidation on perovskite catalysts in the literature. They are named intrafacial and suprafacial respectively [7], depending on the operating temperature. The suprafacial mechanism prevails at low temperature (300 °C) and involves the reaction of surface oxygen adsorbed on the catalyst. The intrafacial mechanism occurs at high temperature (600 °C) when the concentration of adsorbed species becomes low. Bulk oxygen species coming from the perovskite lattice are then believed to be more active and could react with the hydrocarbons. Several parameters can influence the catalytic activity for the deep oxidation of alkanes on perovskites such as specific surface area and amount of oxygen vacancies. The active site is very often thought to be related to the B site. Buciuman et al. [8] reported that the reaction site is most probably associated with manganese cations Mn^{3+} in case of $LaMnO_3$-based catalysts.

In this paper, we present results on the preparation and characterizations of lanthanum manganites and some substituted parents synthesised in nanosized powders. Different compositions of lanthanum manganite nanosized powders were synthesized. The physicochemical properties of the catalysts were characterized by temperature-programmed techniques. The effect of partial substitution on the physicochemical properties of the catalysts characterized by thermal-programmed techniques is discussed. Then, the most suitable composition is selected to be deposited as

* Corresponding author. Tel.: +33 4 72431587; fax: +33 4 72431695.
E-mail address: philippe.vernoux@ircelyon.univ-lyon1.fr (P. Vernoux).

0920-5861/$ – see front matter © 2009 Elsevier B.V. All rights reserved.
doi:10.1016/j.cattod.2009.03.031

thin films on an ionic conductor. As already observed [9] the catalytic activity of doped lanthanum manganites thin films interfaced with an O^{2-} conducting solid electrolyte could be slightly enhanced by using the concept of electrochemical promotion of catalysis (EPOC) also called non-Faradaic electrochemical modification of catalytic activity (NEMCA) effect [10]. This concept, discovered and developed by Vayenas et al. [10], involves the use of an electrochemical catalyst composed of an electronic conductor catalyst and an inert counter electrode both deposited as thin films on each side of a solid electrolyte support. The application of small potentials or currents through the catalyst/electrolyte interface can affect the activity of the catalyst, in a reversible manner. This phenomenon is related to the migration of ions (called promoters) supplied by the current at the surface of the catalyst. The applied polarization is expected to result in a pronounced rate enhancement, superior to the electrochemical rate of supplied ions or ionic current. Indeed, a single ion could activate the reaction of more than one gaseous adsorbed species. The supply or the removal of the promoting ions modifies the binding energy of the reactants on the catalyst. In our previous work [9], the behaviours of strontium substituted lanthanum manganite deposited on Yttria-stabilized zirconia (YSZ) were investigated for the deep oxidation of propane upon anodic polarizations at different temperatures and for various applied potentials. Low electrochemical promotion effects were obtained at temperatures inferiors to 400 °C. The promotional impacts on propane conversion were weak. The magnitude of the effects observed was found to decrease when the temperature and the applied potential increased as it enhanced the oxygen electrochemical reaction kinetic and therefore decreased the lifetime of the promoters on the catalyst. The goal of the present study was to investigate the origins of EPOC on lanthanum manganites deposited on an oxygen ionic conductor via temperature programmed oxidation or reaction as well as solid state electrochemistry characterizations and to link the observed electrochemical promotional effects to the reaction mechanism of propane oxidation on lanthanum manganites.

2. Experimental

2.1. Preparation of lanthanum manganite catalyst powder

Powders of lanthanum manganite, $La_{1-x}Sr_xMnO_3$ ($x = 0$, 0.15 and 0.30), were prepared by a complex route [11] from the thermal decomposition of the chelated nitrate precursors. The following reagents were used $La(NO_3)_3$, $6H_2O$ (p.a. Alfa Aesar), $Sr(NO_3)_2$ (p.a. Acros organics), $Mn(NO_3)_2$, $6H_2O$ (p.a. Alfa Aesar) and maleic acid ($C_4H_4O_4$, p.a. Alfa Aesar). Contents in lanthanum and manganese in the hydrated salts were accurately determined by conventional methods. The nitrate precursors were dissolved in a 10% aqueous solution of maleic acid. Lanthanum nitrate was firstly introduced in the solution, then strontium nitrate was added and finally manganese nitrate. The molar ratio of La/Sr/Mn/maleic acid was the following $1 - x/x/1/8.6$. After the dissolution of the salts, the pH of the mixture was raised at 8 by adding NH_3 solution. Most of the water was then evaporated on a heating plate. The mixture was put overnight in an oven at 130 °C and produced a powder precursor. This last was heated at 500 °C for 2 h to remove the organic compounds and finally calcined at 800 °C for 4 h.

2.2. Powdered catalysts characterizations

XRD measurements were carried out with a Siemens D5005 diffractometer, using the Cu Kα radiation at $\lambda = 0.15418$ nm. The BET specific surface areas of the catalysts were determined from nitrogen adsorption at 77 K by means of a Micromeritics TriStar 3000. Samples were outgassed at 300 °C for 3 h under primary vacuum (using a Micromeritics VacPrep. 061) before pressure measurements.

Temperature programmed desorption of oxygen (O_2-TPD) experiments were performed in a quartz fixed bed reactor with 0.2 g of powder. Each sample was pretreated in oxygen atmosphere at 500 °C for 1 h to adsorb gaseous oxygen on the surface of the catalyst and to remove carbonaceous species from the surface. In the next step, the sample was cooled down to room temperature still under pure oxygen flow. Then, the thermal desorption was carried out by heating the sample at 15 °C min^{-1} from room temperature to 600 °C in pure helium with a flow rate of 1.8 L h^{-1}. Desorption of oxygen was recorded by following the mass 32 with an Infincon transpector-cis mass spectrometer. The surface area of the oxygen desorption peak was calculated with Origin software (OriginLab Corporation) by considering Gaussian peaks.

Temperature programmed reduction (TPR) analyses with hydrogen were carried out on samples (0.1 g) in the reactor used for the O_2-TPD experiments. The catalyst was also pretreated in pure oxygen before running the analysis in the same way as for TPD. Then, TPR was performed with a flow of 1.8 L h^{-1} of 1 vol.% H_2 in He increasing the temperature from room temperature to 650 °C at a heating rate of 10 °C min^{-1}. The reduction profiles were obtained following mass $m/e = 2$ corresponding to H_2 with the mass spectrometer used for the O_2-TPD experiments.

2.3. Preparation of the electrochemical cells

Two types of samples (Fig. 1) were used for the experiments as already described elsewhere [9]. Temperature programmed analyses were performed for propane deep oxidation on an electrochemical catalyst called sample 1 composed of a thin layer of $La_{0.7}Sr_{0.3}MnO_3$ (LSM) (working electrode, W) deposited on one side of a dense YSZ pellet. A gold counter electrode was deposited on the opposite side of the pellet to act as the counter electrode (CE). YSZ pellets were 17 mm in diameter and 1 mm thick. For the electrochemical characterizations, a symmetric sample of LSM/YSZ/LSM was prepared (sample 2). The symmetrical cell was composed of a thick YSZ pellet (diameter = 16 mm and thickness = 1.5 mm) for the electrolyte, with LSM electrodes deposited symmetrically on both sides of the YSZ pellet. Two grids made of gold were used as current collectors. The reference electrode consisted of a silver wire which was fixed on the edge of the YSZ pellet.

The thin film preparation method was developed to obtain reproducible and adherent film of LSM as already reported elsewhere [9].

2.3.1. Characterization of sample 1

The two electrodes W (working electrode LSM), CE (Au counter electrode) were connected to a potensiostat–galvanostat Voltalab PGP 201 (Radiometer Analytical). Catalytic activity measurements under polarization were performed in the potentiostatic mode. The

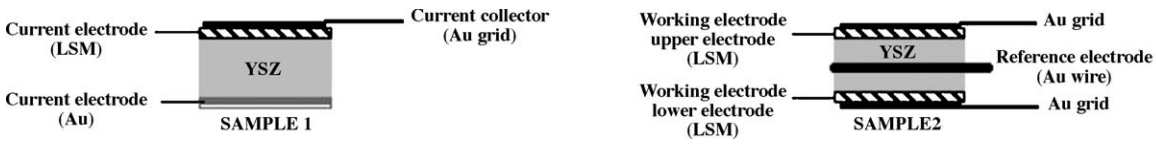

Fig. 1. Schematic drawings of the samples.

Table 1
Specific surface areas, TPD and TPR results of the lanthanum manganite catalyst powders with different strontium contents.

Catalyst	S_{BET} ($m^2\ g^{-1}$)	$T(\alpha)$ (°C) (TPD)	α-O_2 desorbed ($\mu mol\ m^{-2}$)	T_{pic1} (°C) (TPR)	T_{pic2} (°C) (TPR)	T_{pic3} (°C) (TPR)	H_2 consumption ($\mu mol\ g^{-1}$)
$LaMnO_{3+\delta}$	19	290	0.62	212	365	445	1100
$La_{0.85}Sr_{0.15}MnO_{3+\delta}$	22	291	0.73	210	355	420	1200
$La_{0.7}Sr_{0.3}MnO_{3+\delta}$ (LSM)	26	291	1	208	371	480	1200

Faradaic efficiency Λ is defined to quantify the magnitude of the promotion induced by the overpotential as:

$$\Lambda = \frac{r - r_0}{I/nF} \quad (1)$$

where I is the current, n the number of charge carried by the ions and F is the Faraday's constant.

μTemperature programmed desorption of oxygen (O_2-μTPD) was performed on sample 1 in an electrochemical reactor described elsewhere [12]. Oxygen (1% O_2 in He) was adsorbed 1 h at 300 °C either under open circuit conditions (OCV) or upon anodic polarization (+4 V). In the next step, the sample was cooled down to 100 °C still under oxygen flow and polarization to avoid desorption. Then the desorption was carried out with a total He flow rate of 1 L h^{-1} increasing the temperature from 100 to 500 °C at a heating rate of 15 °C min^{-1}. The desorption of oxygen was followed using a μchromatograph (Agilent R3000, SRA Instruments) equipped with two micro-columns (PORAPAQ and molecular sieve) and two micro-TCD. This device enables the analysis of O_2 in 45 s with a detection limit of about 1 ppm. We have checked that only about 475 ppm of O_2 were present in the flowing helium during thermal desorption due to small leak. Let us note that the maximum oxygen partial pressure variation observed during thermal desorption was about 20 ppm.

μTemperature programmed oxidation (μTPO) of propane was also performed on the samples in the same reactor. Propane (8000 ppm in He) was adsorbed 1 h at 300 °C with or without application of a potential to the catalyst. Then, the temperature was decreased to 100 °C still under propane flow and polarization. The reactor was purged under helium flow. Then, the thermal oxidation of propane was carried out by heating the sample at 15 °C min^{-1} from room temperature to 600 °C in O_2 (1% in He) with a flow rate of 1 L h^{-1}. The oxidation of propane on CO_2 was followed using the CO_2 Infra-Red analyzer (Horiba VA 3000).

2.3.2. Electrochemical characterizations of sample 2

Electrochemical measurements were performed on the electrochemical catalysts sample 2 in helium and for different temperatures using an electrochemical interface (Solartron 1286) in a single-chamber type reactor. Therefore the electrode potential was given with respect to the Ag/YSZ reference exposed to residual oxygen in the surrounding atmosphere (i.e. 10^{-4} atm). Unless otherwise specified the potential on the voltammograms corresponds to the applied potential uncorrected from the ohmic drop. The voltammograms were carried out at different sweep rates in the range of 1–50 mV s^{-1} starting either from open circuit conditions (OCV) or following an anodic pretreatment. Three temperatures were investigated: 310, 465 and 495 °C.

Redox potentiometric measurements were also performed with the same experimental setup. This technique developed by Fabry et al. [13] in solid state electrochemistry was used to determine the redox potential of the LSM electrode as a function of the temperature under He. A cathodic potential was initially applied to the sample 2 and the relaxing electrode potential was recorded after current interruption. The relaxation is described as resulting from a slow oxidation of the electrode by the gas phase. If the electrode has been reduced under polarization, the curve may show plateaus or "waves" corresponding to the temporary equilibrium of the different redox system in the oxide.

3. Results

3.1. Characterizations of LSM powders

The X-ray diffraction patterns of the as-prepared catalysts confirm the presence of the pure perovskite rhombohedral phase (ICCD 00-050-0308). The specific surface areas of as-prepared powders were found to be high with values ranging from 19 to 26 $m^2\ g^{-1}$ (Table 1). Similar BET values are reported by Buciuman et al. [8] by using "combustion" synthesis. As already observed in the literature [14], the introduction of strontium in the La sites increased the specific surface area. Indeed, the results reported in Table 1 evidence that the specific area regularly increased from 19 to 26 $m^2\ g^{-1}$ when the strontium level increased from 0 to 30%. SEM pictures (Fig. 2) show rice grain like shapes with numerous necks that indicate some sintering between smaller particles due to the calcination step. The crystallites size was about 40 nm.

Fig. 3 illustrates the standardized O_2-TPD profiles for different Sr contents. Two oxygen desorption peaks were evidenced. The first one takes place at low temperature. The maximum temperature of this peak, denoted as α, is about 290 °C. This α oxygen desorption peak is attributed, in the literature [15–17], to gaseous oxygen adsorbed on the perovskite surface and its intensity is related to the oxygen non-stoichiometry and defect structure of these oxides. The amount of oxygen species involved in this α peak was estimated and normalized per surface unit area. The results are reported in Table 1. It is worth noticing that this low temperature desorption peak is not symmetrical and presents a plateau-like peak at around 400 °C. This was already observed for $LaCoO_3$-based compounds [17] and was ascribed to a second type of α-oxygen species. In good agreement with this result, the α non-symmetrical peak was found to be best fitted with three different

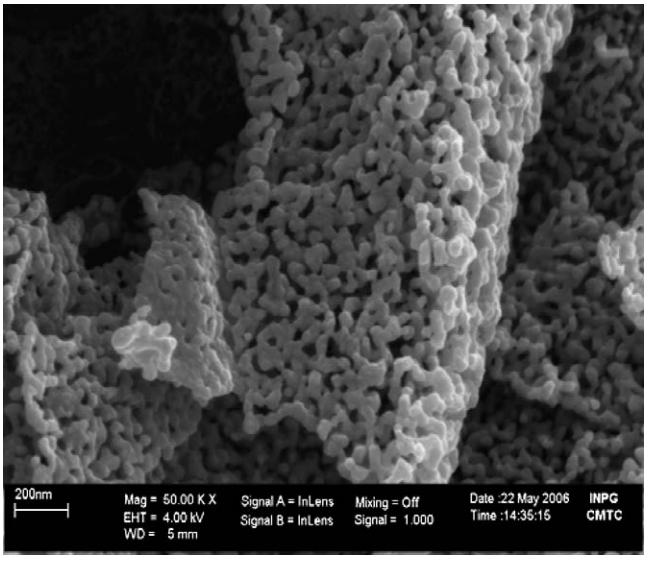

Fig. 2. SEM picture of LSM powder obtained by a complex route.

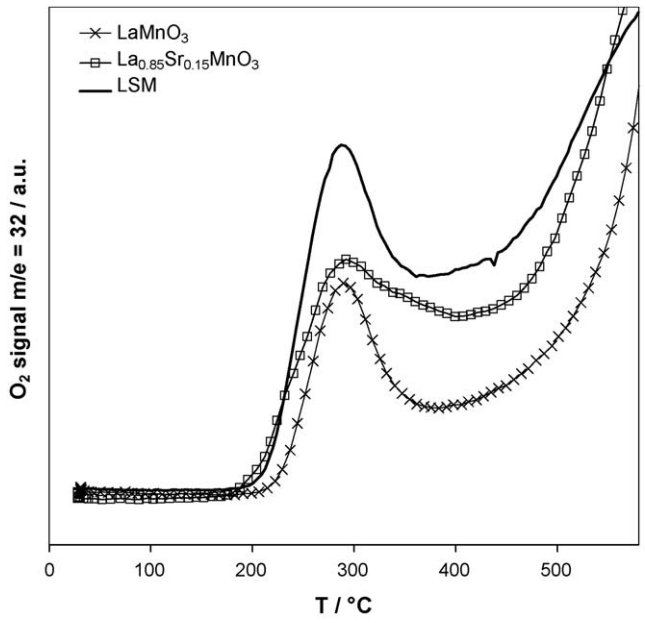

Fig. 3. O_2-TPD profiles of $La_{1-x}Sr_xMnO_3$ powders with different strontium contents. Desorption rate: 15 °C min^{-1}. He flow rate: 1.8 L h^{-1}.

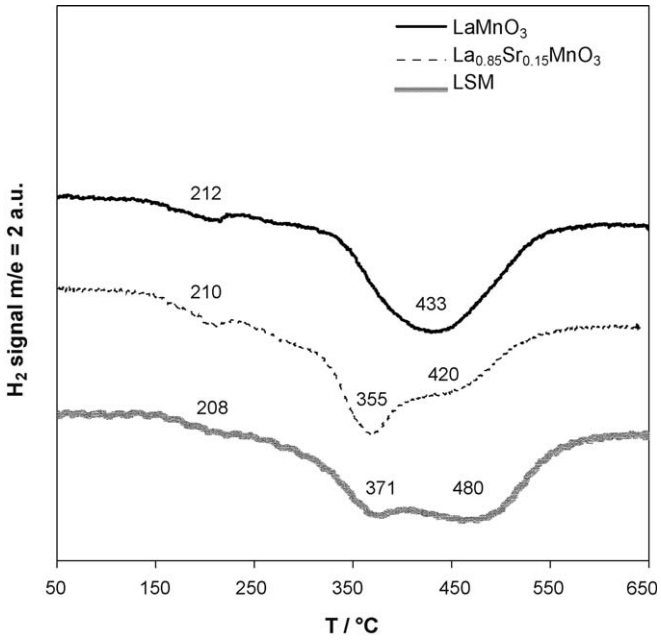

Fig. 4. TPR profiles of $La_{1-x}Sr_xMnO_3$ powders with different strontium contents. Desorption rate: 10 °C min^{-1}. 1% H_2 in He flow rate: 1.8 L h^{-1}.

Gaussian contributions. This could be an indication that different kinds of desorption sites are present on the LSM surface. Nevertheless, it has been difficult to separate the different components of the α peak with a sufficient accuracy. Therefore, only the overall amount of α-oxygen species was determined. Table 1 clearly shows that the amount of α oxygen increases with strontium content. Sample LSM exhibited the highest amount of α oxygen of 1 μmol m^{-2}. The values published by Royer et al. [16] for $LaCoO_3$ agree well with the one calculated here. The level of the plateau at 400 °C increased as *x* varied from 0 to 30%. These results confirm that these oxygen species may be α ones i.e. surface oxygen. Hence the rise of strontium level in perovskite led to an increase of surface oxygen species α. The position of the α oxygen desorption peak did not vary with the Sr content. This suggests that the insertion of strontium enhances the number of oxygen adsorption sites but does not generate a new type. Since the partial substitution of La^{3+} by Sr^{2+} is expected to lead to the formation of oxygen vacancies, one can assume that gaseous oxygen adsorption occurs on this kind of sites. Taking into account the surface area occupied by one oxygen atom as 0.07 nm^2, the coverage of α-oxygen species can be calculated to be around 8.5% for LSM. O_2-TPD spectra exhibit another peak as the signal increased again after the plateau. This β peak was attributed to the desorption of lattice oxygen species, resulting from the reduction of Mn^{4+} to Mn^{3+}. The obtained desorption temperature agrees well with the temperature determined by Teraoka et al. [15]. Those authors [15] reported a thermal reduction in air of tetravalent manganese into trivalent manganese at 535 °C which is close to the onset temperature of the peak obtained in Fig. 3.

Typical reduction profiles recorded on the different catalysts compositions up to 650 °C are exposed in Fig. 4. The spectra baselines were shifted to facilitate comparison between different spectra. Fig. 4 clearly shows the process until the reduction of Mn^{4+} into Mn^{3+} in the 200–500 °C temperature range. The TPR profiles present a small peak, around 200 °C. This peak, denoted as peak 1, could be associated with the surface reduction of Mn^{4+} into Mn^{3+} [18]. The most important part of hydrogen consumption arises in the temperature range 370–500 °C (peaks 2 and 3) and corresponds to the interaction of hydrogen with bulk oxygen species and the simultaneous reduction of Mn^{4+} into Mn^{3+}. The area and the temperature of these two peaks 2 and 3 changes according to the composition of the powder. The TPR profile of $LaMnO_3$ exhibits only one broad peak at 433 °C, nearly symmetric. This peak was found to result from the sum of two Gaussian shaped peaks centred at 365 (peak 2) and 445 °C (peak 3) respectively. The substitution of La^{3+} for Sr^{2+} induces a modification in this profile. Peak 3 weakens for 15% of strontium, a shoulder appears at 420 °C while the peak 2 clearly appeared. For LSM (30% Sr), peak 2 did not move while peak 3 was shifted to higher temperatures. The maximum of peak 2 appeared at 371 °C while the peak 3 was found at 480 °C. We suggest that peaks 2 and 3 could be linked to two different Mn(IV)–O chemical bonds in the perovskite structure. Spinicci et al. [19] measured the electrical conductivity of $LaMnO_3$ during oxygen adsorption/desorption and evidenced oxygen surface species, O^- or O_2^-, which would be easily available and mobile. Furthermore, these authors associated the existence of these mobile oxygen species with the presence of Mn^{4+}. The amount of H_2 consumed per gram of catalyst was calculated (Origin software). The results are reported in Table 1. The same amount of H_2 was found for $La_{0.85}Sr_{0.15}MnO_3$ and LSM corresponding to a similar amount of Mn^{3+} (or Mn^{4+}) and it was higher than for $LaMnO_3$.

In summary LSM exhibited the highest amount of oxygen vacancies, the highest specific surface area and H_2 consumed during TPR experiments. Therefore this composition was selected to be deposited as thin films on YSZ to perform EPOC experiments.

3.2. Characterizations of LSM/YSZ

3.2.1. Electrochemical characterizations

Cyclic voltammetry was performed to observe modification of the oxidation state of manganese supposed to be linked to the active site in LSM as proposed by Van Rosmalen et al. [14]. At 310 °C voltammograms were recorded starting from −0.5 V up to 0.5 V and for different scan rates in the range of 1–30 mV s^{-1} as depicted in Fig. 5(a). The sample was pretreated under 0.5 V for 1 min before recording the experiments. No oxidation or reduction peak was observed. As expected from a capacitive behaviour the voltammograms evidenced a current plateau which varied with the scan rate. Fig. 5(b) shows the variation of the current plateau

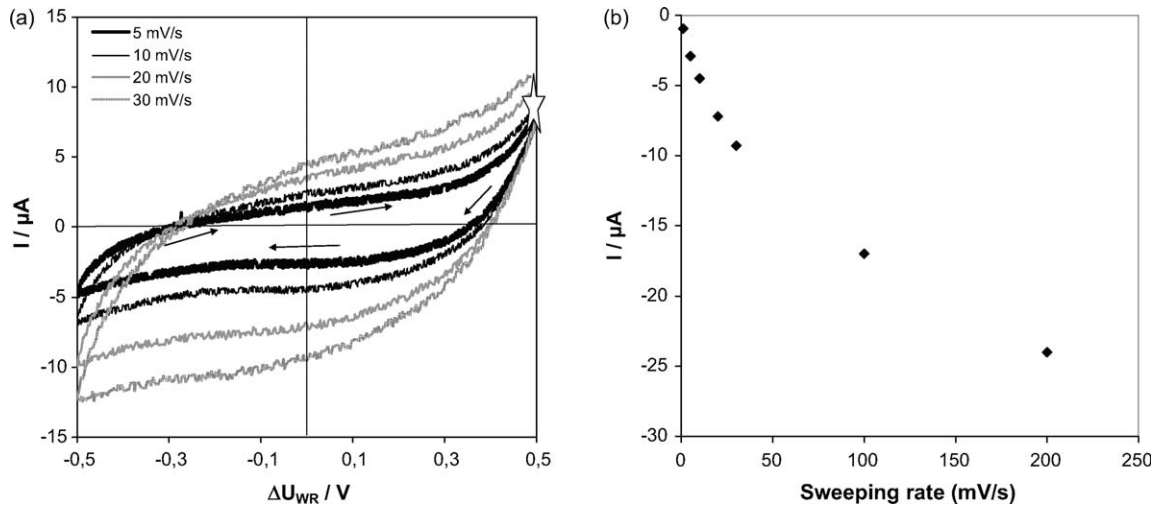

Fig. 5. (a) Cyclic voltammetry recorded at 300 °C on LSM/YSZ under He for different scan rates. (b) Influence of the sweep rate on the capacitive current corresponding to the plateau on the cathodic scan of the voltammogram.

with the scan rate. This current was estimated during the cathodic scan. As expected it became more negative as the scan rate was increased from 1 to 200 mV s^{-1}. However the variation was not linear indicating that the capacitance was not constant. The order of magnitude of the capacitance was estimated from the slopes of the curve in Fig. 5(b). It is in the range of 10^{-4} to 10^{-3} F cm^{-2}. This order of magnitude is higher than that expected from the double layer capacitance at the Pt/YSZ interface resulting from the Helmholtz model [20]. Such huge capacitance values can be explained by charge storage in the form of chemical species called "pseudo-capacity" as proposed by Schouler and Kleitz [21]. In the present case, we suggest that this capacity is linked to the oxygen adsorption on the LSM surface and is related to the phenomenon of oxygen backspillover at the LSM/gas interface. The higher value of the capacitance observed when the scan rate was decreased favours this interpretation. The presence of pseudo capacitive processes related to oxygen backspillover has also been recently proposed by Jaccoud et al. [22] to explain charge storage in the O_2, Pt/YSZ system at 450 °C. Fig. 6(a) shows a typical voltammetric response obtained at 460 °C for a scan rate of 1 mV s^{-1} (grey curve). The catalyst was pretreated at +1.5 V for 10 min before recording the cathodic and reverse scan. Two reduction peaks called PC1 and PC2 and two oxidation peaks denoted PA1 and PA2 appeared. The separation of the two oxidation peaks seems more difficult when increasing the scan rate to 40 mV s^{-1} (Fig. 6(a) black curve). The shape of the reduction peak PC2 was also modified by the scan rate change. The scan rate modifies the kinetics of the redox processes and therefore influenced the oxidation and reduction peaks. The four peaks which were observed at high scan rate at 460 °C could readily be seen at 495 °C with a scan rate of 1 mV s^{-1}. Fig. 6(b) compares two voltammograms recorded for a scan rate of 1 mV s^{-1} at 465 and 495 °C. The potential was varied from open circuit value to cathodic potentials down to −2 V and up to +1.5 V to return to its initial open circuit values. Two cycles were recorded at each temperature. During the first cathodic scan the black curve recorded at 465 °C exhibited one reduction peak (PC1) and one broad oxidation peak during the reverse scan. The reduction peak PC2 only appeared during the second cycle i.e. after the potentials values had reached +1.5 V. This could be an indication that peak PC2 is the reduction of oxidized species formed at high anodic potentials. Hence the oxidation peaks PA1 and PA2 seem to be linked to PC1. When the reversed potential was higher than −1 V,

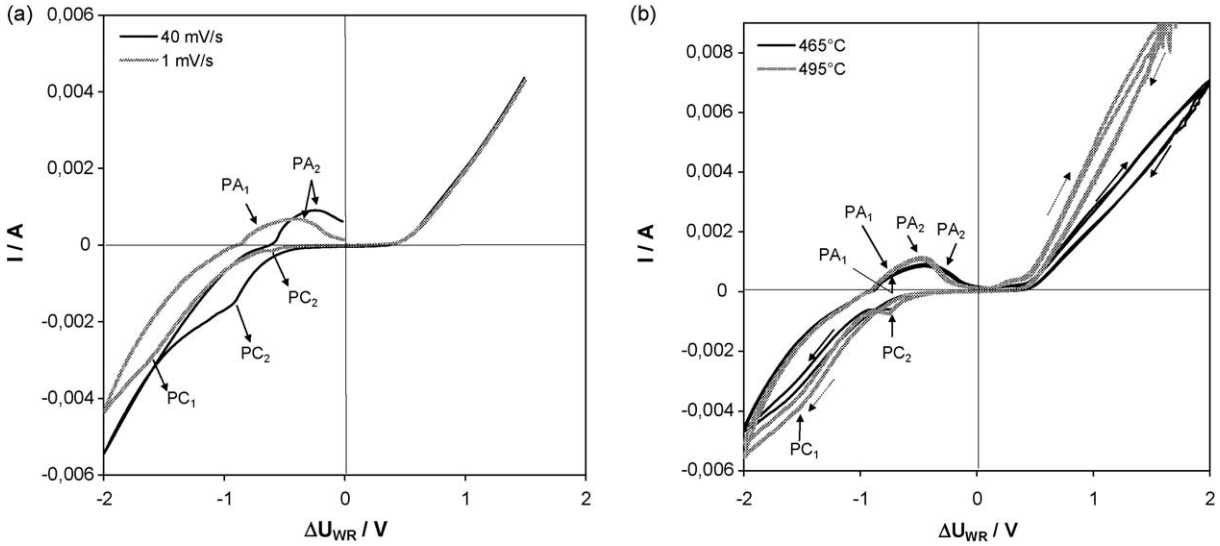

Fig. 6. Typical voltammetric response of the LSM/YSZ electrode under helium 3 L h^{-1}. (a) Influence of the scan rate on the cyclic voltammogram recorded after 10 min polarization at +1.5 V at 460 °C. (b) Voltammograms recorded for a scan rate of 1 mV s^{-1} at 465 and 495 °C.

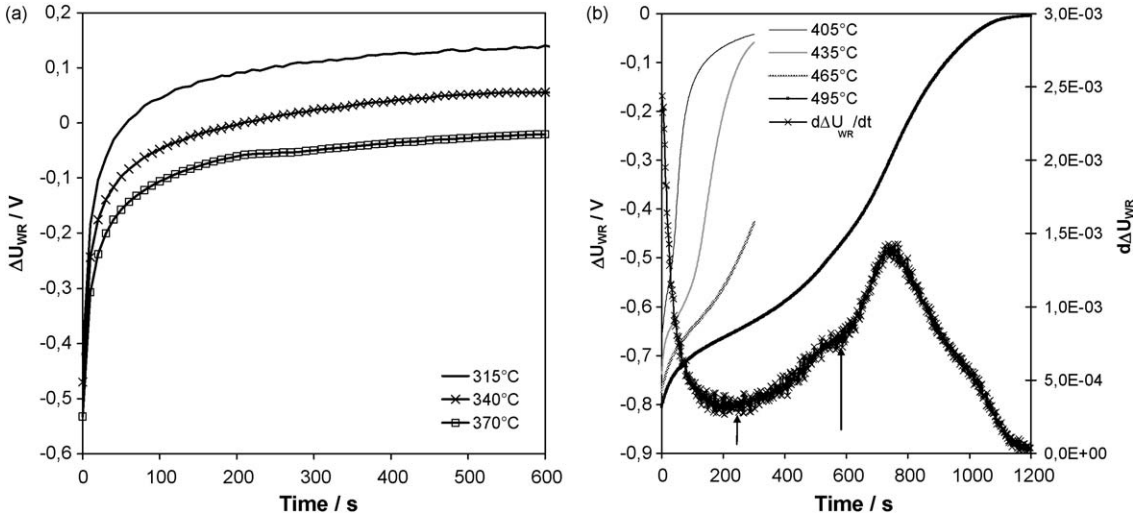

Fig. 7. Influence of the temperature on the relaxation of the LSM electrode under OCV after polarization at −1.5 V for 2 min. He flow 3 L h^{-1}.

PA1 was not observed. This indicates that the PA2 process is faster than PA1 one. The grey curve recorded at 495 °C shows the same behaviour. In this case the two contributions PA1 and PA2 appeared more clearly. Thus it can be proposed that two redox processes are evidenced in LSM since two reoxidation peaks may be observed in the voltammograms under certain conditions. Those two processes occur in the same potential range. As a consequence they cannot be easily separated.

Redox potentiometric measurements were also performed to confirm the interpretation of the voltammetric response and to try to determine the redox potential in LSM. Fig. 7 shows the relaxation potentiometric response of the LSM/YSZ electrode under OCV conditions after polarization at −1.5 V for 2 min. The curves were plotted as a function of the temperature in the temperature range of 300–500 °C. As seen from Fig. 7(a), below 400 °C, no wave or inflexion point was observed on the curve suggesting that no redox process occurred at these temperatures as already observed by cyclic voltammetry. It is worth mentioning that the open circuit potential corresponding to the stabilization was not equal to zero. This potential was therefore not fixed by the oxygen electrode reaction in this temperature range. When the temperature exceeded 400 °C (Fig. 7(b)), a wave was observed on the relaxation curve at 405, 435 and 465 °C. However the determination of the corresponding potential of the inflexion point value was not easy in good agreement with the bad separation of peaks PA1 and PA2 observed by cyclic voltammetry. At 495 °C two waves appeared. The corresponding inflexion points were about −0.65 and −0.5 V. This potential was determined by plotting the derivative $d\Delta U_{WR}(t)/dt$ as a function of the time of the curve in Fig. 7(b) (minima are indicated by arrows). This result is consistent with the existence of two redox processes in LSM as already observed by cyclic voltammetry when the temperature and the scan rates increase. Moreover, potentials at the inflexion points seem to correspond to those of PA1 and PA2 observed by cyclic voltammetry (Fig. 6(b)). Let us note that in this temperature range, the open circuit potential was equal to zero indicating that it was fixed by the oxygen electrode reaction. The difference between the two potentials at the inflexion points is low (−0.15 V). This is in the same range as the difference between PA1 and PA2 at 495 °C. Those two redox processes with very close potentials values would correspond to the Mn^{4+}/Mn^{3+} redox couple. Backhaus-Ricoult et al. [23] reported 0.15 V/10^{-4} atm for the thermodynamic potential of Mn^{4+}/Mn^{3+} corresponding to the MnO_2/Mn_2O_3 equilibrium. The values determined in the present work are lower indicating that Mn^{4+} is less easily reduced to Mn^{3+} in LSM that in MnO_2. It is noteworthy that they are higher than the potential determined in [23] for the stability of LSM. This confirms that the peaks on the voltammetric response involve processes in LSM which retains the perovskite structure.

3.2.2. μTemperature programmed desorption

In situ O_2-μTPD experiments were recorded on LSM/YSZ to observe the influence of the electrical polarization on the adsorption strength of oxygen on the catalyst as depicted in Fig. 8(a). The black curve refers to the desorption spectrum obtained after adsorption of pure oxygen under OCV. The baseline under 1 L h^{-1} of helium was 475 ppm of O_2. The desorption profiles show one broad peak between 180 and 300 °C. The amount of oxygen desorbed was very low about 20 ppm at maximum. The maximum temperature of this peak was centred at about 270 °C. The area of this peak was estimated to correspond to 0.099 μmol O_2 and therefore to 0.19 μmol O_2 m^{-2} (m_{LSM} = 20 mg on LSM/YSZ). This value is in the same range as the one obtained on the powdered catalysts (Table 1). The grey curve in Fig. 8(a) was recorded on the same sample after oxygen adsorption upon polarization of +4 V corresponding to a current of about 143 μA. Let us note that in this case the gaseous adsorption of oxygen and the polarization occurred simultaneously as for EPOC experiments. The TPD spectra exhibit the same shape. The position of the maximum of the α oxygen desorption peak was quite similar for the two curves. The amount of oxygen desorbed was a little lower, about 15 ppm corresponding to 0.084 μmol O_2. This difference was not significant enough and correspond to our measurements uncertainties.

3.2.3. μTemperature programmed oxidation of propane

μTPO confirmed the adsorption of propane on LSM: two peaks appeared on the TPO spectra, one at low temperature (below 300 °C) and another one in the range of 500–600 °C (Fig. 8(b)). For an adsorption of propane under OCV (black curve), propane oxidation started at 111 °C and the maximum of the first peak was at 217 °C. The area of this peak was 0.2 μmol CO_2. If we assume that CO_2 was provided exclusively by the reaction of chemisorbed propane with gaseous oxygen, then this value would correspond to 0.063 μmol C_3H_8 adsorbed. After the first peak, the CO_2 concentration decreased but did not return to its initial value and a second peak appeared centred at 468 °C. These two peaks could correspond to propane molecule and carbonaceous compounds derivated from propane polymerization, both adsorbed on LSM surface. We assumed that the first peak was due to propane

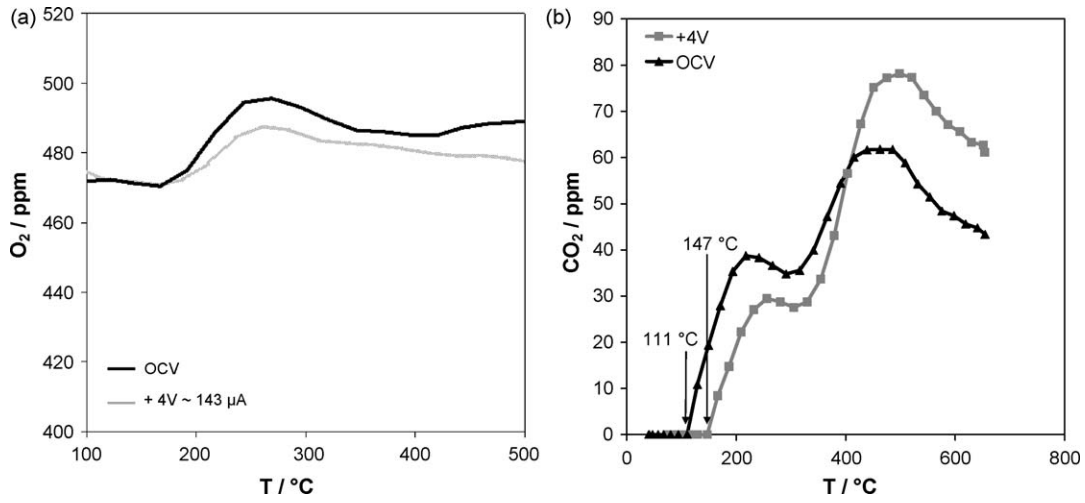

Fig. 8. (a) O_2-μTPD profiles of LSM/YSZ under open circuit conditions and upon +4 V. Desorption rate: 15 °C min^{-1}. He flow rate: 1 L h^{-1}. (b) μTPO profiles of LSM/YSZ under open circuit conditions and upon +4 V. Desorption rate: 15 °C min^{-1}. O_2 flow rate: 1 L h^{-1}.

molecules weakly adsorbed which can react with oxygen. The same TPO profile was observed when propane was adsorbed under +4 V. The current during propane adsorption was quite stable about 15 μA. We checked that no CO_2 was produced during propane adsorption possibly due to propane electrochemical oxidation. The CO_2 curve started to increase at 147 °C and the maxima of the two peaks were at 256 and 498 °C. Hence an anodic polarization of +4 V during the adsorption of propane shifted the peaks to higher temperature and delayed propane oxidation. It also decreased the area of this low temperature peak to 0.15 μmol CO_2. However the area of the second peak increased sharply. This suggests that a positive polarization could modify the reactivity of chemisorbed propane and the repartition of the adsorption sites. Under TPO conditions, propane deep oxidation into CO_2 started at extremely low temperatures, i.e. 110 and 145 °C for a prior propane adsorption upon OCV and +4 V, respectively, suggesting a weak propane adsorption on LSM (Fig. 8(b)). Such low propane oxidation temperatures were achieved thanks to the prior adsorption of propane before feeding the oxygen. This seems to indicate that the rate-limiting step in propane deep oxidation is the adsorption of propane in competition with oxygen. Nevertheless, additional characterizations by Raman and FTIR are necessary to identify carbonaceous compounds generated by propane adsorption on LSM.

4. Discussion

The possibility of controlling in situ the catalytic activity of LSM for the deep oxidation of propane by applying anodic polarizations was already observed in a previous study [9] but with weak promotional effects. Electrochemical characterizations showed high electrochemical performances of the LSM electrode. Weak overpotentials were measured and a small non-Faradaic zone was observed during anodic cyclic voltammetry. EPOC was reported only when the temperature was decreased below 400 °C.

In the present study electrochemical characterizations and TPR experiments show that no redox process appears in LSM below 300 °C. When the temperature exceeded 400 °C, broad oxidation and reduction peaks were observed on the cyclic voltammetry corresponding to a wave on the relaxation potentiometric curve with an inflection point. TPR experiments exhibit between 370 and 500 °C one broad peak with two maxima assigned to the reduction of two Mn^{4+} with different environments. Voltammetry results could be related to the same process in LSM. The species reduced during PC1 would be reoxidized during PA1 and PA2 at close potentials but with different rates. Peak PA2 was more clearly observed at high scan rate. Therefore the corresponding electrochemical process is supposed to have a higher rate than that corresponding to PA1. Peak PA2 was also observed at high temperature in agreement with the existence of two inflexion points on the relaxation potentiometric curve. Therefore it can be concluded that at temperature higher than 400 °C, two reduction processes take place in LSM occurring respectively at close temperatures in the TPR experiments and close potentials in the electrochemical measurements. They could be related to the reduction of Mn^{4+} with two different environments. Furthermore at $T < 400$ °C, the open circuit potential was not zero so it was not fixed by the oxygen electrode reaction. While for $T > 400$ °C, it was fixed by this reaction suggesting a fast reaction rates in this temperature range in good agreement with the low lambda values found on LSM/YSZ during EPOC experiments in a previous study [9]. Let us notice that the Faradaic efficiency value is linked to the ratio of the lifetime of ionic oxygen species and oxygen species coming from the gas phase. The kinetic of promoter consumption on LSM may be fast, and then the lifetime of the promoter at the surface of the catalyst may be short. For $T > 400$ °C no EPOC was observed. This could be related to the high reactivity at the triple phase boundary. The origin of EPOC observed in the literature on metal/YSZ electrochemical catalysts is attributed to the migration of ions on the catalyst/gas interface upon polarization. The presence of those ions could modify the adsorption strength of adsorbates at the surface of the catalyst. μTPD experiments investigated the influence of polarization at 300 °C on the absorption strength of oxygen on LSM. Let us note that these μTPD experiments are, to the best of our knowledge, the first ones carried out at atmospheric pressure on pelleted samples (17 mm diameter) and on perovskite film interfaced with YSZ. Low temperature desorption peak of oxygen was observed during TPD experiments on LSM/YSZ. The temperature of desorption was quite closed to the one obtained on LSM powder (290 °C). Hence, this peak denoted α oxygen desorption peak, could be attributed to adsorption of gaseous oxygen on oxygen vacancies at the surface of the perovskite. Furthermore, the quantity of these α-oxygen species was found to be closed to that found on powdered catalysts (Table 1). Oxygen was adsorbed either upon anodic polarization or open circuit conditions. Several authors [24–26] reported a shift of the maximum temperature of desorption to lower temperatures upon anodic polarization conditions on Pt/YSZ. This was ascribed to the formation of more reactive oxygen species due to the presence of backspillover oxygen at the metal-gas interface. They

assumed that this could be at the origin of EPOC on Pt/YSZ. In our study the position of the maximum of the desorption peak was the same upon polarization and open circuit conditions. This result suggests that the electrical polarization during adsorption process has no significant impact on gaseous oxygen chemisorption on LSM thin films. This is in agreement with the interpretation that ionic oxygen (promoters) has a very short lifetime. On the other hand, we cannot also exclude that promoting ions could also have been supplied thermally under OCV in this temperature range as suggested by Karoum et al. [27] on Pt/YSZ. Nevertheless in both case supplying promoters has no influence on the binding strength of oxygen on LSM. The temperature range of propane oxidation (i.e. 220–260 °C) corresponds to the maximum temperature of desorption of α oxygen (i.e. 270–290 °C). This result suggests quite similar binding strength of propane and oxygen on LSM. TPO showed that prior adsorption of propane without oxygen led to very low oxidation temperatures. Hence we can assume that propane adsorption should be the rate-determining step of the oxidation process. Furthermore, an anodic polarization of +4 V during the propane adsorption was found to shift the peaks to higher temperatures. We assume that the first peak could be attributed to propane adsorbed on LSM whereas the second would correspond to the polymerization of carbonaceous species at the surface of LSM. Anodic polarization seems to encourage this polymerization as the maximum of CO_2 concentration was higher. This result indicates an increase in the adsorption strength of propane on LSM. This could lead in propane/O_2 reactive mixture to an increase of the propane coverage on LSM. Therefore, this modification of propane chemisorption on LSM could be at the origin of the slight electrochemical promotional effects observed on LSM/YSZ at 300 °C.

In summary, at 300 °C it was possible to observe an influence of the polarization on the binding strength of propane on LSM which could slightly increase the propane coverage on LSM and then the catalytic activity. Rate enhancement ratio of 1.25 was reported at 300 °C in a previous study [9] with corresponding Faradaic efficiency of the order of 5 (25% conversion gain). However, at this temperature the oxidation state of manganese cannot be modified by the polarization, then limiting the magnitude of EPOC. On the other hand, for $T > 400$ °C the polarization could influence the oxidation state of manganese and therefore the ratio Mn^{3+}/Mn^{4+} and then the catalytic performances as trivalent manganese cations are supposed to be the active sites. Unfortunately, in this temperature range, the oxygen evolution reaction is too fast and therefore the lifetime of the promoters on LSM was too low to observe any EPOC, as experimentally reported [9].

5. Conclusions

This study presents physicochemical characterizations of lanthanum manganites both as powdered catalysts and thin films interfaced on YSZ pellets. Temperature-programmed techniques (O_2-TPD, TPR and TPO) as well as cyclic voltammetry and potentiometric measurements were carried out in order to elucidate the origins of electrochemical promotion of propane deep oxidation observed on LSM/YSZ electrochemical catalyst. Temperature-programmed techniques have shown that oxygen chemisorption on LSM is not significantly modified by a positive polarization, whereas the binding strength of propane on LSM was found to be strengthened. This last observation could enhance the propane coverage and then explain slight electrochemical promotional effects evidenced at 300 °C. Electrochemical characterizations have revealed that the polarization can modify the Mn^{3+}/Mn^{4+} ratio from 400 °C, this redox couple being at the origin of the catalytic activity. Unfortunately, from 400 °C, the oxygen evolution electrode becomes so fast that the O^{2-} species lifetime becomes too small to observe any EPOC.

Acknowledgments

Financial supports by the CNRS and IFP as well as by the European Marie-Curie EFEPOC project (MSCF-CT-2006-046201) are gratefully acknowledged.

References

[1] M.F.M. Zwinkels, S.G. Jaras, P.G. Menon, Catal. Rev. Sci. Eng. 35 (3) (1993) 319.
[2] H. Arai, T. Yamada, K. Eguchi, T. Seiyama, Appl. Catal. 26 (1986) 265.
[3] P. Ciambelli, S. Cimino, L. Lisi, M. Faticanti, G. Minelli, I. Pettiti, P. Porta, Appl. Catal. B 33 (2001) 193.
[4] N.H. Batis, P. Delichere, H. Batis, Appl. Catal. A 282 (2005) 173.
[5] B.P. Barbero, J.A. Gamboa, L.E. Cadus, Appl. Catal. B 65 (2006) 21.
[6] P. Ciambelli, S. Cimino, S. De Rossi, L. Lisi, G. Minelli, P. Porta, G. Russo, Appl. Catal. B 29 (2001) 239.
[7] R.J.H. Voorhoeve, in: J.J. Burton, R.L. Garten (Eds.), Advanced Materials in Catalysis, Academic Press, New York, 1977, p. 129.
[8] F.C. Buciuman, F. Patcas, J.C. Menezo, J. Barbier, T. Hahn, H.G. Lintz, Appl. Catal. B 35 (2002) 175.
[9] V. Roche, E. Siebert, M.C. Steil, J.P. Deloume, C. Roux, T. Pagnier, R. Revel, P. Vernoux, Ionics 14 (3) (2008) 235.
[10] C.G. Vayenas, S. Bebelis, C. Pliangos, S. Brosda, D. Tsiplakides, Electrochemical Activation of Catalysis: Promotion, Electrochemical Promotion and Metal–Support Interactions, Kluwer Academic/Plenum Publishers, New York, 2001.
[11] D. Berger, V. Fruth, I. Jitaru, J. Schoonman, Mater. Lett. 58 (2004) 2418.
[12] P. Vernoux, F. Gaillard, L. Bultel, E. Siebert, M. Primet, J. Catal. 208 (2002) 412.
[13] P. Fabry, M. Kleitz, C. Deportes, J. Solid State Chem. 5 (1972) 1.
[14] J.A.M. Van Rosmalen, J.P.P. Huijsmans, E.H.P. Cordfunke, Solid State Ionics 66 (1993) 285.
[15] Y. Teraoka, M. Yoshimatsu, N. Yamazoe, T. Seyama, Chem. Lett. (1984) 893.
[16] S. Royer, F. Berube, S. Kaliaguine, Appl. Catal. A 282 (2005) 273.
[17] H.M. Zhang, Y. Shimizu, Y. Teraoka, N. Miura, N. Yamazoe, J. Catal. 121 (1990) 432.
[18] S. Ponce, M.A. Pena, J.L.G. Fierro, Appl. Catal. B 24 (2000) 193.
[19] R. Spinicci, M. Faticanti, P. Martini, S. De Rossi, P. Porta, J. Mol. Catal. A 197 (2003) 147.
[20] B.L. Kuzin, D.I. Bronin, Solid State Ionics 136–137 (2000) 45.
[21] E. Schouler, M. Kleitz, J. Electroanal. Chem. 64 (1975) 135.
[22] A. Jaccoud, C. Falgairette, G. Foti, C. Comninellis, Electrochim. Acta 52 (2007) 7927.
[23] M. Backhaus-Ricoult, K. Adib, T. St Clair, B. Luersen, L. Gregoratti, A. Barinov, Solid State Ionics 179 (2008) 891.
[24] X. Li, F. Gaillard, P. Vernoux, Top. Catal. 4 (2007) 391.
[25] D. Tsiplakides, S.G. Neophytides, C.G. Vayenas, Ionics 7 (2001) 203.
[26] A. Katsaounis, Z. Nikopoulou, X.E. Verykios, C.G. Vayenas, J. Catal. 222 (2004) 192.
[27] R. Karoum, A. de Lucas-Consuegra, F. Dorado, J.L. Valverde, A. Billard, P. Vernoux, J. Appl. Electrochem. 38 (2008) 1083.